An Examination of the Reaction Pathways for the HOOOBr and HOOBrO Complexes Formed from the HO_2 + BrO Reaction

Sujata Guha and Joseph S. Francisco*

Department of Chemistry and Department of Earth & Atmospheric Sciences, Purdue University, West Lafayette, Indiana 47907-1393

Received: June 9, 1999; In Final Form: August 10, 1999

The geometries, vibrational spectra, and relative energetics of the $HBrO_3$ isomers (HOOOBr and HOOBrO) and their transition states have been examined by using the quadratic configuration interaction method in conjunction with various basis sets. From the dissociation energies of the $HBrO_3$ isomers, it is found that the most energetically favorable process during the HO_2 + BrO reaction pathway is the formation of HOOBrO as an intermediate, and its eventual dissociation into HOBr and O_2, due to the very low energy barrier (2.8 kcal mol^{-1}) involved. The HOOOBr species, if formed as an intermediate, will be more likely to dissociate into HBr + O_3 rather than HOBr + O_2, as the energy barrier for the latter process is quite high (26.4 kcal mol^{-1}) relative to the energy barrier for the HOOOBr → HBr + O_3 dissociation process.

I. Introduction

Among all the halogens that are present in sufficient amounts in the stratosphere, bromine is the most effective species that participates in efficient catalytic cycles leading to destruction of the ozone layer. In spite of the fact that bromine compounds are much less abundant than chlorine compounds in the stratosphere, it has been estimated that the chemistry involving bromine species is responsible for ∼25% of the ozone loss observed in Antarctica[1] and up to 40% of ozone loss during winter in the Arctic region.[2] The efficiency of bromine in destroying ozone is greatly enhanced by its synergistic coupling reaction with chlorine compounds, leading to the production of bromine and chlorine atoms:[3]

$$BrO + ClO \rightarrow Br + Cl + O_2 \quad (1)$$

The most abundant bromine-containing source gas is methyl bromide, present mainly due to oceanic biological processes. Methyl bromide is used for fumigation, has a very high ozone depletion potential, and is scheduled to be phased out in developed countries by the year 2010.[4] Other important bromine source gases that reach the stratosphere include tetrabromobisphenol A and trifluoromethyl bromide, used as fire retardants and refrigerants.

The coupling of bromine oxides with HO_x species (such as OH and HO_2 radicals) to destroy ozone has been of particular significance. A critical reaction that couples BrO_x and HO_x species in the gas-phase catalytic cycle of bromine is the reaction between BrO and HO_2. This process should increase the recycling of bromine radicals, and could be efficient in regions with significant OH concentration profiles.

$$Br + O_3 \rightarrow BrO + O_2 \quad (2)$$

$$BrO + HO_2 \rightarrow HOBr + O_2 \quad (3)$$

$$HOBr + h\nu \rightarrow OH + Br \quad (4)$$

$$OH + O_3 \rightarrow HO_2 + O_2 \quad (5)$$

Net:
$$2O_3 \rightarrow 3O_2 \quad (6)$$

Experimental results have suggested that reaction 3 proceeds at a substantially faster rate than had been indicated by previous measurements, and may play a major role in the ozone-related chemistry of bromine compounds.

The reaction between BrO and HO_2 radicals has two thermodynamically feasible channels:

$$BrO + HO_2 \rightarrow HOBr + O_2 \qquad \Delta H^\circ_{r,298} = -45.1 \text{ kcal mol}^{-1} \quad (3a)$$

$$\rightarrow HBr + O_3 \qquad \Delta H^\circ_{r,298} = -7.7 \text{ kcal mol}^{-1} \quad (3b)$$

The first study of this reaction was performed by Cox and Sheppard using the molecular-modulation UV absorption technique.[5] BrO and HO_2 were produced by photolysis of O_3 in the presence of Br_2, HO_2, and O_2 and analyzed directly by UV absorption. The rate constant was determined as 5×10^{-12} cm^3 $molecule^{-1}$ s^{-1} at 303 K and 760 Torr total pressure. A similar value of the rate constant was suggested by Baulch et al. for use in atmospheric modeling.[6] Poulet et al. performed a more direct study by means of the discharge flow mass spectrometric method, determined a much higher value of the rate constant than was obtained by Cox and Sheppard, and observed HOBr as the only product at 298 K.[7] The higher rate constant value has been confirmed by flash photolysis and UV absorption studies of $Br_2/O_3/Cl_2/CH_3OH/O_2$/He mixtures, carried out by Hayman et al.[8] and Bridier at al.[9] at 298 K and 760 Torr. The fair agreement among the three determinations suggested a value around $k_3 = 3 \times 10^{-11}$ cm^3 $molecule^{-1}$ s^{-1} at 298 K for the BrO + HO_2 reaction. Larichev et al.[10] used discharge flow mass spectrometry to investigate the kinetics and mechanism of the BrO + HO_2 reaction in the temperature range 233−344 K, and observed HOBr to be the major product. They obtained a rate constant value of $(4.77 \pm 0.32) \times 10^{-12}$ cm^3 $molecule^{-1}$ s^{-1}, and observed a negative temperature dependence, suggesting the presence of an $HBrO_3$ complex. Elrod et al. conducted experiments which reported a much smaller rate constant value, $(1.4 \pm 0.3) \times 10^{-11}$ cm^3 $molecule^{-1}$ s^{-1}, at 298 K.[11] Recently, Cronkhite et al. conducted laser flash photolysis studies of Cl_2/

10.1021/jp9918961 CCC: $18.00
Published on Web 09/18/1999

$CH_3OH/O_2/Br_2/O_3/N_2$ mixtures and determined the rate constant of the $BrO + HO_2 \rightarrow HOBr + O_2$ reaction to be $(2.0 \pm 0.6) \times 10^{-11}$ cm^3 molecule^{-1} s^{-1} at 296 K.[12] Their observations support the lower values of k_3 reported by Elrod et al.[11] over the higher values of k_3 reported by Poulet et al.,[7] Bridier et al.,[9] and Larichev et al.[10]

Mellouki et al. tried to measure the yield of the HBr-forming channel from the $BrO + HO_2$ reaction, and determined an upper limit on the yield of HBr by measuring an upper limit for the rate coefficient of the reverse reaction, $HBr + O_3 \rightarrow HO_2 + BrO$.[13] The limits measured at 300 and 441 K were extrapolated to low temperatures, and the yield of HBr was determined as being negligible (<0.01%) throughout the stratosphere. Mellouki et al. also observed a negative temperature dependence for the $BrO + HO_2$ reaction, suggesting the presence of an $HBrO_3$ complex.[13] Garcia and Solomon reported a theoretical analysis of the BrO atmospheric measurements database using a two-dimensional photochemical model, and concluded that the $BrO + HO_2$ reaction could not have a significant yield of HBr.[14] Li et al. performed experimental studies of the $BrO + HO_2$ reaction over the temperature range 233−348 K using discharge flow mass spectroscopy.[15] They found that, at 298 K, the rate coefficient was $(1.73 \pm 0.6) \times 10^{-11}$ cm^3 molecule^{-1} s^{-1} with excess HO_2 and $(2.05 \pm 0.64) \times 10^{-11}$ cm^3 molecule^{-1} s^{-1} with excess BrO.

Guha and Francisco[16] examined the possibility of $HBrO_3$ complexes that could be formed from the $BrO + HO_2$ reaction, following the suggestion of Mellouki et al.[13] The ordering of energy among the $HBrO_3$ isomeric forms that could be formed during the $BrO + HO_2$ reaction has been found to be $HOBrO_2 < HOOOBr < HOOBrO < HBrO_3$,[16] with all isomers (except $HBrO_3$) lying at a lower energy level than $BrO + HO_2$. Li et al. proposed that, for $HOBrO_2$ to be formed from the reaction of BrO and HO_2 radicals, there has to exist an energy barrier as required by the observed negative activation energy for reaction 3.[15] Thus, reaction channel 3a probably proceeds via the initial formation of HOOBrO and the subsequent formation of a cyclic transition state intermediate, which decomposes to form $HOBr + O_2$. As predicted, HOOBrO is weakly bound, while HOOOBr is 75 kcal mol^{-1} more stable than the reactant radicals, $BrO + HO_2$.[16] Due to the very small observed value for k_{3b}/k_3, it is proposed that there must exist a significant energy barrier toward conversion of HOOOBr to $HBr + O_3$ via the formation of another cyclic transition state intermediate,[12] and such a proposal requires further investigation.

In this paper we present *ab initio* molecular orbital calculation results of the structures, vibrational spectra, and relative energetics of the transition states of the HOOBrO and HOOOBr isomers. Such a study enables us to determine whether there exist significant energy barriers for the conversion of HOOOBr $\rightarrow HBr + O_3$ (or $HOBr + O_2$), and HOOBrO $\rightarrow HOBr + O_2$ via the formation of cyclic transition state intermediates. A knowledge of the energy barriers is extremely important in ascertaining the exact pathways of formation of the products, $HOBr + O_2$ and $HBr + O_3$, during the process of reaction of BrO and HO_2 radicals.

II. Computational Methods

Ab initio molecular orbital calculations were performed using the GAUSSIAN 94 program.[17] The equilibrium geometries of HOOOBr and HOOBrO isomers and their transition states were fully optimized to better than 0.001 Å for bond distances, and 0.1° for bond angles, with a self-consistent field convergence of at least 10^{-9} on the density matrix. The QCISD (Quadratic Configuration Interaction with Single and Double excitations) method[18] was used with the 6-31G(d,p) and 6-311G(d,p)[19] basis sets in the optimization of the geometries for the equilibrium and transition state structures. A second set of polarization functions supplemented the latter basis set to comprise the 6-311G(2d,2p) basis set, with which optimizations were also performed. The harmonic vibrational frequencies and intensities of all species were calculated at the QCISD level of theory in conjunction with the 6-31G(d,p) basis set, using the geometries calculated at the QCISD/6-31G(d,p) level of theory. To improve the energies, single point calculations were performed with the QCISD(T) (Quadratic Configuration Interaction with Single and Double excitation incorporating the perturbative corrections for Triple excitation) wave functions, using the optimized geometries obtained at the QCISD/6-311G(2d,2p) level of theory.

III. Results and Discussion

A. Geometries and Vibrational Frequencies. Computations on the HOOOBr and HOOBrO isomeric forms and the transition states were performed using the QCISD method in conjunction with the 6-31G(d,p), 6-311G(d,p), and 6-311G(2d,2p) basis sets. In general, the structures optimized using the highest basis set [6-311G(2d,2p)] are found to be in good agreement with those computed using the other two basis sets. The calculated structures of the HOOOBr and HOOBrO isomeric forms agree well with our former optimizations of those structures at the CCSD(T)/TZ2P level of theory.[16] The structural parameters for HOOOBr, HOOBrO, and the transition states are provided in Table 1a.

The straight-chain structure of HOOOBr is skewed, with the HOOO′ and OOO′Br dihedral angles being 75.9° and 80.9°, respectively, at the QCISD/6-311G(2d,2p) level of theory. The HOO and OO′Br angles are predicted to be 101.2° and 110.0°, respectively. The OOO′ angle (107.5°) is smaller than the OO′Br angle (110.0°) due to the greater repulsion between the lone electron pairs on the bromine atom of HOOOBr and those on the oxygen atom, compared to the repulsion between the lone electron pairs on the two oxygen atoms. Interestingly enough, a comparison of the O−O and O−O′ bond lengths of HOOOBr (1.422 Å and 1.401 Å, respectively) with the O−O length in HOOBr (1.405 Å)[20] reveals that the bonding between the two species is quite similar. The H−O length in HOOOBr (0.963 Å) is much smaller than the O−O and O−O′ bond lengths, due to the larger overlap between the 1s orbital of the small hydrogen atom and the 2p orbital of the comparatively larger oxygen atom, versus the overlap between the two equal-sized oxygen atoms. However, there is poorer overlap between the 3d orbital of the large bromine atom with the 2p orbital of oxygen, compared to the overlap between the 2p orbitals of the two oxygen atoms, making the O′−Br length larger (1.884 Å) than the O−O and O−O′ lengths.

The other isomeric form, HOOBrO, too has a straight-chain structure, but with oxygen as a terminal atom. The minimum-energy structure for HOOBrO is nonplanar, skewed. The dihedral angle between the HOOBr atoms is 99.1°, while that between the OOBrO′ atoms is 79.5°. The OBrO′ angle (110.6°) is a little larger than the OOBr angle (109.2°). As in the case of HOOOBr, for HOOBrO, the HOO angle (100.8°) is smaller than the OOBr angle, due to the greater degree of repulsion between the two lone pairs of electrons on bromine and those on the oxygen atoms. The O−Br bond distance decreases from 1.929 Å, when the smallest [6-31G(d,p)] basis set is used, to 1.883 Å, when the largest [6-311G(2d,2p)] basis set is used, indicating that the size of the basis set affects the bond lengths.

TABLE 1: Optimized Geometries (Angstroms and Degrees) for (a) HOOOBr, HOOBrO, and Their Transition States and (b) Reactants and Products

species	coordinates	level of theory		
		QCISD/6−31G(d,p)	QCISD/6−311G(d,p)	QCISD/6−311G(2d,2p)
	(a) HOOOBr, HOOBrO, and Their Transition States			
HOOO′Br	*r*(OO′)	1.409	1.383	1.401
	r(O′Br)	1.911	1.915	1.884
	r(OO)	1.436	1.417	1.422
	r(HO)	0.972	0.966	0.963
	∠(OO′Br)	109.7	110.9	110.0
	∠(OOO′)	107.3	108.1	107.5
	∠(HOO)	101.0	101.4	101.2
	∠(OOO′Br)	79.5	82.2	80.9
	∠(HOOO′)	75.3	76.3	75.9
HOOBrO′	*r*(OBr)	1.929	1.926	1.883
	r(BrO′)	1.704	1.691	1.674
	r(OO)	1.441	1.419	1.437
	r(HO)	0.970	0.964	0.962
	∠(OBrO′)	110.8	111.7	110.6
	∠(OOBr)	109.0	110.3	109.2
	∠(HOO)	100.9	101.3	100.8
	∠(OOBrO′)	77.8	80.3	79.5
	∠(HOOBr)	96.5	99.2	99.1
[HOOO′Br → HBr + O_3]‡	*r*(OO′)	1.303	1.249	1.245
	r(OO)	1.389	1.363	1.377
	r(HBr)	1.592	1.678	1.701
	r(HO)	1.364	1.220	1.194
	∠(OOO′)	110.8	111.3	111.5
	∠(HOO)	94.5	96.9	97.1
	∠(BrHO)	152.9	157.4	158.9
	∠(HOOO′)	−39.9	−41.1	−40.0
	∠(BrHOO)	−8.9	−13.6	−21.5
[HOOO′Br → HOBr + O_2]‡	*r*(O′Br)	1.810	1.805	1.788
	r(OO′)	2.294	2.273	2.266
	r(OO)	1.296	1.271	1.277
	r(HO)	0.993	0.987	0.988
	∠(HOO)	101.4	102.3	101.8
	∠(OOO′)	83.0	79.2	81.3
	∠(BrO′O)	98.9	126.8	114.5
	∠(HOOO′)	−29.3	−32.3	−45.3
	∠(OOOBr)	117.1	113.4	111.4
[HOOBrO′ → HO′Br + O_2]‡	*r*(BrO′)	1.766	1.755	1.741
	r(OO)	1.357	1.331	1.342
	r(HO′)	1.342	1.393	1.326
	r(HO)	1.095	1.063	1.099
	∠(HO′Br)	96.7	97.5	96.7
	∠(HOO)	101.7	102.6	101.6
	∠(O′HO)	144.9	142.6	148.0
	∠(OHO′Br)	40.5	38.8	34.5
	∠(BrHOO)	−54.3	−55.7	−48.2
	(b) Reactants and Products			
HO_2	*r*(HO)	0.974	0.969	0.966
	r(OO)	1.353	1.333	1.342
	∠(HOO)	103.8	104.4	103.8
BrO	*r*(BrO)	1.781	1.777	1.754
HOBr	*r*(HO)	0.969	0.962	0.960
	r(BrO)	1.869	1.866	1.848
	∠(HOBr)	102.0	101.9	102.4
$O_2(^1\Delta)$	*r*(OO)	1.233	1.212	1.218
HBr	*r*(HBr)	1.443	1.417	1.417
O_3	*r*(OO)	1.275	1.256	1.261
	∠(OOO)	117.4	117.7	117.6

There is also a similar trend in the Br−O′ bond length which decreases with increased basis set size. The other structural parameters, such as the H−O and O−O bond lengths, are not significantly influenced by enlargement of the basis set. The H−O length (0.962 Å) is smaller than the O−O length (1.437 Å) due to the better overlap between the small 1s orbital of hydrogen and the relatively larger 2p orbital of oxygen. For the different levels of theory used, the O−Br bond lengths are larger than the Br−O′ lengths. The lone electron pairs on the terminal oxygen atom of HOOBrO sometimes tend to resonate with the Br−O′ bonding electron pairs, due to which the Br−O′ bond attains a partial double-bond character. This resonance effect is not observed with the oxygen atom that is sandwiched between the hydrogen and bromine atoms. Thus, the Br−O′

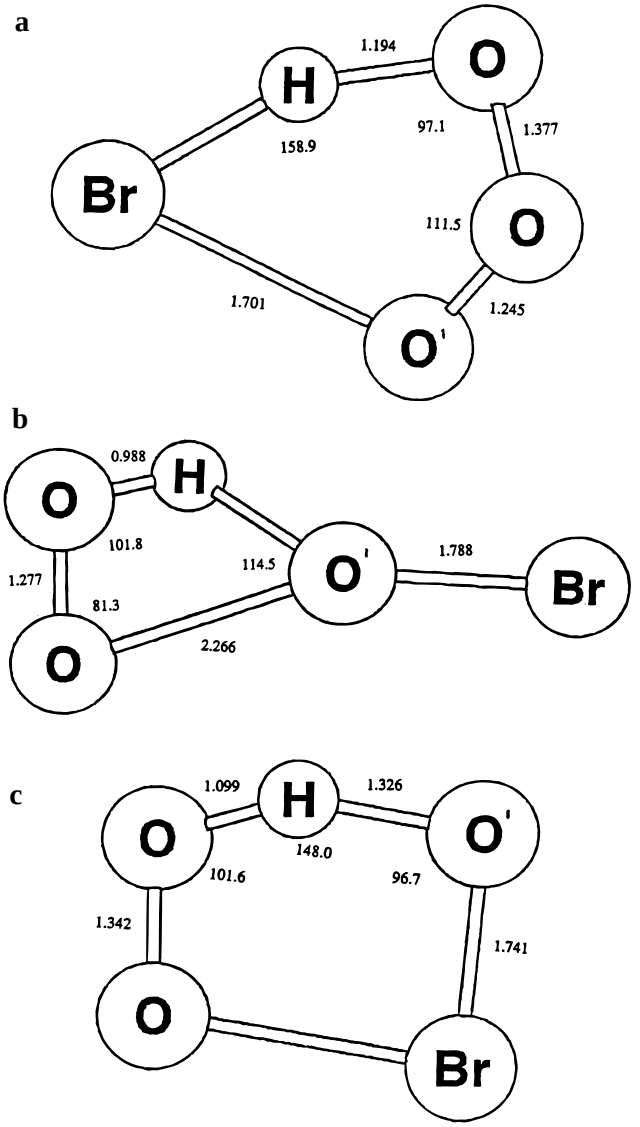

Figure 1. Transition states for HOOOBr and HOOBrO dissociation. (a) HOOOBr → HBr + O_3 transition state. (b) HOOOBr → HOBr + O_2 transition state. (c) HOOBrO → HOBr + O_2 transition state.

bond, with its partial double-bond character, is smaller (1.674 Å) than the O−Br single bond (1.883 Å).

Among the three transition states, the first is [HOOOBr → HBr + O_3]‡, whose structure is shown in Figure 1a. This transition state leads to the conjunction of the bromine atom with the hydrogen atom to form HBr and the residual ozone. Due to this phenomenon, there are certain interesting structural changes that are observed when a comparison is made of the HOOOBr → HBr + O_3 transition state structure to the structure of the stable HOOOBr species. At the 6-311G(2d,2p) level of theory, the O−O′ bond length decreases from 1.401 Å in HOOOBr to 1.245 Å in [HOOOBr → HBr + O_3]‡. The H−O bond length in HOOOBr is slightly smaller (0.963 Å) than that in the [HOOOBr → HBr + O_3]‡ structure (1.194 Å), while the O−O bond length in HOOOBr (1.422 Å) is slightly larger. There is an H−Br bond, 1.701 Å long, present in the HOOOBr → HBr + O_3 transition state structure, that is not present in the structure of the stable HOOOBr species. There are observable changes in the bond angles between the two structures, too. For HOOOBr, the OOO′ angle is 107.5°, while for [HOOOBr → HBr + O_3]‡ the OOO′ angle is larger (111.5°). The HOO angle in the [HOOOBr → HBr + O_3]‡ structure is smaller (97.1°) than the corresponding angle in HOOOBr (101.2°).

Figure 1b shows the structure of the second transition state, HOOOBr → HOBr + O_2, that leads to the migration of the bromine atom to join the oxygen atom (attached to the hydrogen) to form HOBr and elimination of the residual oxygen. As in the case of the former transition state, there are certain differences observed between the structural parameters of HOOOBr and [HOOOBr → HOBr + O_2]‡. The O−O′ length increases markedly from 1.401 Å in HOOOBr to 2.266 Å in [HOOOBr → HOBr + O_2]‡. The H−O length (0.963 Å) in HOOOBr is slightly smaller than that (0.988 Å) in the [HOOOBr → HOBr + O_2]‡ structure. The O′−Br bond length decreases from 1.884 Å in HOOOBr to 1.788 Å in the HOOOBr → HOBr + O_2 transition state. The bond angles between the stable and transition state species are also different. The OOO′ angle decreases significantly from 107.5° in HOOOBr to 81.3° in [HOOOBr → HOBr + O_2]‡. There are increases in the HOO and OO′Br angles in going from HOOOBr to the HOOOBr → HOBr + O_2 transition state.

The third and final transition state structure is that of HOOBrO → HOBr + O_2, as depicted in Figure 1c. In this structural form, the bromine atom migrates to join the oxygen attached to the hydrogen to form HOBr. The structure of this transition state possesses some notable differences from that of the stable HOOBrO species. There is a slight increase in the Br−O′ length in going from HOOBrO (1.674 Å) to [HOOBrO → HOBr + O_2]‡ (1.741 Å). The O−O length decreases slightly from 1.437 Å in HOOBrO to 1.342 Å in [HOOBrO → HOBr + O_2]‡, while the H−O length increases to 1.099 Å in the transition state structure. The HOO angle is also larger (101.6°) in the [HOOBrO → HOBr + O_2]‡ structure, compared to the HOO angle (100.8°) in HOOBrO.

The calculated harmonic vibrational frequencies and intensities of HOOOBr, HOOBrO, and the transition states are provided in Table 2a. The frequencies and intensities for the reactants and products of the HO_2 + BrO reaction process are listed in Table 2b. The vibrational frequencies are obtained at the QCISD level of theory in conjunction with the 6-31G(d,p) basis set.

For HOOOBr, the most intense band is predicted to be the HOOO′ torsion (437 cm^{-1}), followed by the HOO bend (1435 cm^{-1}) and H−O stretch (3726 cm^{-1}), while the least intense bands are the OOO′ bend (587 cm^{-1}) and the BrO′OO torsion (131 cm^{-1}). The H−O stretch and HOO bend observed for HOOOBr occur with almost the same frequencies as the H−O stretch and HOO bend in the HO_2 reactant radical (listed in Table 2b). However, the O−O and Br−O stretches in HOOOBr occur at lower frequencies (928 and 517 cm^{-1}, respectively) relative to the O−O and Br−O stretches in HO_2 and BrO, due to the conformational changes that take place when the HOOOBr intermediate is formed. The Br−O′ stretching frequency occurring at 517 cm^{-1} is much lower than the frequencies of the H−O and O−O stretches, consistent with the longer Br−O′ bond length compared to the H−O and O−O bond lengths (see Table 1). The harmonic frequencies of HOOOBr are very similar to those obtained by Francisco and Sander for HOOOCl,[21] except that the Br−O′ stretch is predicted to occur at a lower frequency than the Cl−O stretch, and the BrO′O bend is predicted to occur at a lower frequency than the ClOO bend (consistent with the larger mass of bromine relative to chlorine). The modes involving bromine in HOOOBr are smaller in their infrared intensities compared to the analogous modes involving chlorine.

TABLE 2: Harmonic Frequencies (cm^{-1}) and Intensities (km mol^{-1}) for (a) HOOOBr, HOOBrO, and Their Transition States and (b) Reactants and Products

(a) HOOOBr, HOOBrO, and Their Transition States

			QCISD/6-31G(d,p)	
species	mode no.	mode description	frequencies	intensities
HOOO′Br	1	HO stretch	3726	40
	2	HOO bend	1435	48
	3	OO stretch	928	31
	4	OO′ stretch	851	24
	5	OOO′ bend	587	6
	6	BrO′ stretch	517	25
	7	HOOO′ torsion	437	91
	8	BrO′O bend	295	11
	9	BrO′OO torsion	131	4
HOOBrO′	1	HO stretch	3734	43
	2	HOO bend	1441	49
	3	OO stretch	962	58
	4	BrO sym bend	801	25
	5	BrO asym str	476	74
	6	H-wag	444	34
	7	BrOO bend	268	1
	8	OBrO′ bend	192	10
	9	torsion	38	3
$[HOOO'Br \rightarrow HBr + O_3]^{\ddagger}$	1	HO stretch	1380	42
	2	HBr stretch	1028	149
	3	OO stretch	851	193
	4	HOO bend	787	28
	5	OO′ stretch	646	29
	6	OOO′ bend	411	6
	7	BrHO bend	318	11
	8	HOOO′ torsion	140	150
	9	reaction coord	1416i	235
$[HOOO'Br \rightarrow HOBr + O_2]^{\ddagger}$	1	HO stretch	3359	1435
	2	HOO bend	1530	127
	3	OO stretch	947	1911
	4	OO′ stretch	649	125
	5	BrO′ stretch	594	135
	6	BrO′O bend	293	13
	7	OOO′ bend	147	3
	8	OOO′Br torsion	73	0
	9	reaction coord	1049i	5411
$[HOOBrO' \rightarrow HO'Br + O_2]^{\ddagger}$	1	HO stretch	1926	118
	2	HO′ stretch	1445	51
	3	OO stretch	1010	39
	4	HOO bend	705	21
	5	HOBr bend	519	18
	6	OHO′Br torsion	475	8
	7	BrO stretch	274	11
	8	O′HO bend	196	6
	9	reaction coord	961i	112

(b) Reactants and Products

				QCISD/6-31G(d,p)	
species	symmetry	mode no.	mode description	frequencies	intensities
HO_2	a	1	HO stretch	3619	14
		2	HOO bend	1470	46
		3	OO stretch	1178	22
BrO	a	1	BrO stretch	715	4
HOBr	a	1	HO stretch	3851	62
		2	HOBr bend	1211	48
		3	BrO stretch	615	4
$O_2(^1\Delta)$	a	1	OO stretch	1460	0
HBr	a	1	HBr stretch	2712	3
O_3	a	1	OO stretch	1266	0
		2	OOO bend	725	7
	a′	3	OO stretch	1043	369

The harmonic frequencies of HOOBrO are a little lower in magnitude relative to the frequencies of its chlorinated counterpart HOOClO.[21] For HOOBrO the most intense bands are the Br−O asymmetric stretch occurring at a frequency of 476 cm^{-1} and the O−O stretch occurring at 962 cm^{-1}, while the least intense band is the BrOO bending mode at 268 cm^{-1}. The H−O and O−O stretching frequencies (3734 and 962 cm^{-1}, respectively) are much larger than the Br−O stretching fre-

TABLE 3: Total and Single Point Energies[a] (hartrees) for (a) HOOOBr, HOOBrO, and Their Transition States and (b) Reactants and Products in the HO_2 and BrO Reaction

(a) HOOOBr, HOOBrO, and Their Transition States

level of theory	HOOOBr	HOOBrO	[HOOOBr → HBr + O_3]‡	[HOOOBr → HOBr + O_2]‡	[HOOBrO → HOBr + O_2]‡
QCISD/6−31G(d,p)	−2795.488 03	−2795.446 81	−2795.432 09	−2795.418 84	−2795.443 03
QCISD/6−311G(d,p)	−2798.085 46	−2798.038 16	−2798.031 57	−2798.017 62	−2798.035 98
QCISD/6−311G(2d,2p)	−2798.145 51	−2798.101 78	−2798.091 51	−2798.077 01	−2798.100 78
QCISD(T)/6−311G(2d,2p)[a]	−2798.179 10	−2798.145 76	−2798.137 52	−2798.134 83	−2798.141 66
QCISD(T)/6−311++G(2df,2p)[a]	−2798.293 91	−2798.269 51	−2798.247 06	−2798.248 14	−2798.260 24
QCISD(T)/6−311++G(3df,3pd)[a]	−2798.320 66	−2798.297 58	−2798.275 01	−2798.275 53	−2798.289 09

(b) Reactants and Products in the HO_2 + BrO Reaction

level of theory	HO_2	BrO	HOBr	$O_2(^1\Delta)$	HBr	O_3
QCISD/6−31G(d,p)	−150.530 84	−2644.932 41	−2645.586 76	−149.898 98	−2570.596 08	−224.847 61
QCISD/6−311G(d,p)	−150.605 30	−2647.458 44	−2648.116 49	−149.973 07	−2573.105 05	−224.954 45
QCISD/6−311G(2d,2p)	−150.641 12	−2647.483 54	−2648.142 21	−150.004 47	−2573.109 22	−225.005 37
QCISD(T)/6−311G(2d,2p)[a]	−150.654 03	−2647.493 59	−2648.154 86	−150.023 76	−2573.113 33	−225.044 99
QCISD(T)/6−311G(2df,2p)[a]	−150.704 46	−2647.557 68	−2648.219 17	−150.073 53	−2573.146 75	−225.123 50
QCISD(T)/6−311++G(3df,3pd)[a]	−150.714 32	−2647.574 28	−2648.238 46	−150.080 85	−2573.162 48	−225.135 20

[a] Calculated using the QCISD/6-311G(2d,2p) geometries.

quency (476 cm^{-1}), since the H−O and O−O bond lengths are much smaller than the Br−O bond length. There are similar differences in the O−O and Br−O stretching frequencies between HOOBrO and the HO_2 and BrO radicals, as was observed in the case of HOOOBr. There is a hydrogen-wag mode observed at a frequency of 444 cm^{-1} for HOOBrO that is not observed for HOOOBr.

The first transition state structure is that of [HOOOBr → HBr + O_3]‡, whose frequencies can be compared to the frequencies of the stable HOOOBr species. The [HOOOBr → HBr + O_3]‡ structure has one imaginary frequency, suggesting that the transition state structure is a first-order saddle point. The H−O stretch in [HOOOBr → HBr + O_3]‡ occurs at a much lower frequency (1380 cm^{-1}) than the H−O stretch in HOOOBr (3726 cm^{-1}), consistent with the slightly larger H−O length in the transition state structure than in HOOOBr. The O−O and O−O′ stretches in HOOOBr occur at higher frequencies than the corresponding O−O and O−O′ stretches in [HOOOBr → HBr + O_3]‡. The HOO bend in the [HOOOBr → HBr + O_3]‡ transition state structure occurs at a much lower frequency (787 cm^{-1}) than the HOO bend in HOOOBr (1435 cm^{-1}).

The second transition state structure is that of [HOOOBr → HOBr + O_2]‡, for which there also appears to be an imaginary frequency. The frequencies of the [HOOOBr → HOBr + O_2]‡ structure also reveal certain differences when compared to the frequencies of HOOOBr, due to the structural differences between the two conformations. The Br−O′ stretch in [HOOOBr → HOBr + O_2]‡ occurs at a larger frequency (594 cm^{-1}) than the corresponding Br−O′ stretch in HOOOBr (517 cm^{-1}), consistent with the shorter Br−O′ length in the [HOOOBr → HOBr + O_2]‡ transition state. The H−O stretching frequency of [HOOOBr → HOBr + O_2]‡ is a little bit lower than the H−O stretch in HOOOBr. The O−O stretch possesses a higher frequency in [HOOOBr → HOBr + O_2]‡ than HOOOBr, due to its shorter bond length in the transition state structure. Due to the changes in conformation between the [HOOOBr → HOBr + O_2]‡ and [HOOOBr → HBr + O_3]‡ transition states, the Br−O′ stretch and BrO′O bend mode are observed in [HOOOBr → HOBr + O_2]‡, while they are absent in [HOOOBr → HBr + O_3]‡.

The final transition state structure is that of [HOOBrO → HOBr + O_2]‡ which, characteristic of all transition states, has an imaginary frequency. The structure of [HOOBrO → HOBr + O_2]‡ differs to some extent from that of the stable HOOBrO species. The Br−O stretch in HOOBrO occurs at a higher frequency (476 cm^{-1}) than the Br−O stretch in the HOOBrO → HOBr + O_2 transition state (274 cm^{-1}), due to the shorter Br−O length in HOOBrO. The O−O bond is longer in HOOBrO than in [HOOBrO → HOBr + O_2]‡, and thus the O−O stretch in [HOOBrO → HOBr + O_2]‡ occurs at a higher frequency (1010 cm^{-1}) compared to that in HOOBrO (962 cm^{-1}). The H−O bond length in HOOBrO is shorter than the H−O and H−O′ lengths in [HOOBrO → HOBr + O_2]‡, and thus the H−O stretch in HOOBrO possesses higher frequency. The HOBr bend, present in the [HOOBrO → HOBr + O_2]‡ conformation, is not observed for HOOBrO. Similarly, the OBrO′ bend, present at 192 cm^{-1} in HOOBrO, disappears during the HOOBrO → HOBr + O_2 transition.

B. Relative Energetics of $HBrO_3$ Isomers and Transition States. The total energies of the $HBrO_3$ intermediates and the transition states calculated at the QCISD level of theory, using the 6-31G(d,p), 6-311G(d,p), and 6-311G(2d,2p) basis sets, are provided in Table 3a. The table also lists the single point energy data which are obtained from calculations performed at the QCISD(T) level of theory with the 6-311G(2d,2p), 6-311++G(2df,2p), and 6-311++G(3df,3pd) basis sets, employing the optimized geometries obtained at the QCISD/6-311G(2d,2p) level of theory. In Table 3b are listed the total and single point energy values for the reactants (HO_2 and BrO) and possible products (HOBr, O_2, HBr, and O_3), which are used in calculating the heats of reaction of the three transition states. Table 4 contains information about the heats of reaction and heights of the energy barriers for the [HOOOBr → HBr + O_3]‡, [HOOOBr → HOBr + O_2]‡, and [HOOBrO → HOBr + O_2]‡ transition states at the QCISD and QCISD(T) levels of theory using various basis sets. Zero-point energy changes are incorporated in the highest level [QCISD(T)/6-311++G(3df,3pd)] of calculated single point energy values. Table 5 provides the heats of formation for the reactants and products involved in the HO_2 + BrO reaction.

From Table 3a it is observed that, at all levels of computation, the HOOOBr structural form possesses lower energy and is more stable than the HOOBrO structure. This observation is consistent with our earlier predictions[16] of the relative energetic stability among the $HBrO_3$ isomers. The heat of reaction for the process of HO_2 + BrO going to HOOOBr, according to our earlier

TABLE 4: Relative Energetics (kcal mol^{-1}) for the Products and Transition States in the HO_2 + BrO Reaction

level of theory	$[HO_2 + BrO \rightarrow HOOOBr]^{\ddagger}$ $\Delta H^{\circ}_{r,0}$	$[HOOOBr \rightarrow HBr + O_3]^{\ddagger}$ $\Delta H^{\circ}_{r,0}$	barrier height	$[HOOOBr \rightarrow HOBr + O_2]^{\ddagger}$ $\Delta H^{\circ}_{r,0}$	barrier height	$[HOOBrO \rightarrow HOBr + O_2]^{\ddagger}$ $\Delta H^{\circ}_{r,0}$	barrier height
QCISD/6−31G(d,p)	−15.5	27.8	35.1	1.5	43.4	−24.4	2.4
QCISD/6−311G(d,p)	−13.6	16.3	33.8	2.6	42.6	−32.3	1.4
QCISD/6−311G(2d,2p)	−13.1	19.4	33.9	0.7	43.0	−28.2	0.6
QCISD(T)/6−311G(2d,2p)	−19.8	13.0	26.1	0.3	27.8	−20.6	2.6
QCISD(T)/6−311++G(2df,2p)	−19.9	14.8	29.4	0.8	28.7	−14.6	5.8
QCISD(T)/6−311++G(3df,3pd)	−20.1	14.4	28.6	0.8	28.3	−13.6	5.3
ΔZPE	2.8	−4.5	−4.8	−2.2	−1.9	−1.4	−2.5
QCISD/(T)/6−311++G(3df,3pd) + ΔZPE	−17.3	9.9	23.8	−1.4	26.4	−15.0	2.8

TABLE 5: Heats of Formation (0 K) for Species in the HO_2 + BrO Reaction[a,b]

species	$\Delta H^{\circ}_{f,0}$ (kcal mol^{-1})
$O_2(^1\Delta)$	0.0
O_3	34.7 ± 0.2
HOBr	−10.93 ± 1
HBr	−6.8 ± 1
BrO	31.8 ± 0.5
HO_2	4.3 ± 1.2

[a] Chase, M. W.; Davies, C. A.; Downey, J. R.; Frurip, D. J.; McDonald, R. A.; Syverud, A. N. *J. Phys. Chem. Ref. Data Suppl.* **1985**, *1*. [b] Ruscic, R.; Berkowitz, J. *J. Chem. Phys.* **1994**, *101*, 7795.

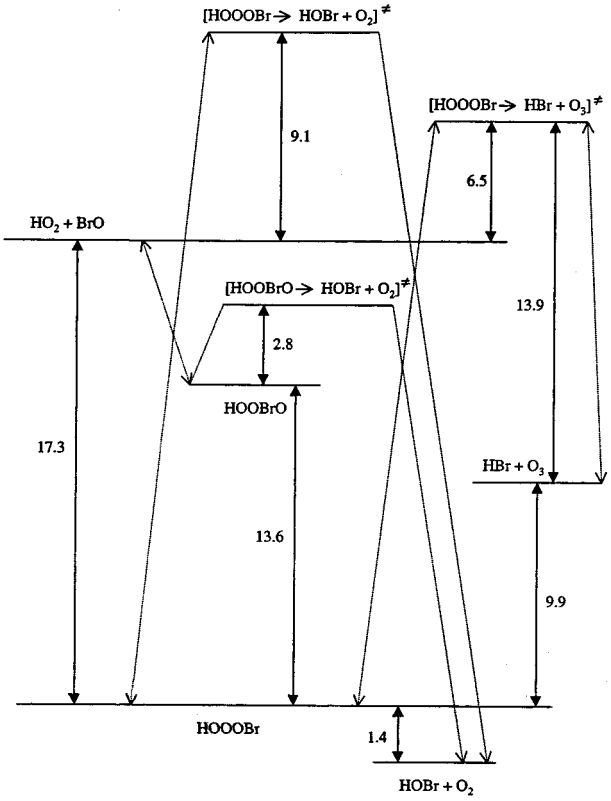

Figure 2. Relative energetics of the HO_2 + BrO reaction.

prediction,[16] is −17.9 kcal mol^{-1} at the CCSD(T)/6-311++G-(3df,3pd)//CCSD(T)/TZ2P level of theory. Our present calculations estimate the heat of reaction for the same process to be −17.3 kcal mol^{-1} at the QCISD(T)/6-311++G(3df,3pd)//QCISD/6-311G(2d,2p) level of theory. From Table 4 it is observed that the best estimates of the heats of reaction for the HOOOBr → HBr + O_3, HOOOBr → HOBr + O_2, and HOOBrO → HOBr + O_2 transition states are 9.9, −1.4, and −15.0 kcal mol^{-1}, respectively, at the QCISD(T)/6-311++G-(3df,3pd) level of theory. The highest energy barrier (26.4 kcal mol^{-1}) is possessed by the HOOOBr → HOBr + O_2 transition state, whereas the HOOBrO → HOBr + O_2 transition state has the lowest energy barrier (2.8 kcal mol^{-1}). The HOOBrO → HOBr + O_2 transition state structure lies at a much lower energy level relative to the HOOOBr → HOBr + O_2 and HOOOBr → HBr + O_3 transition state structures and is, thus, more stable.

Figure 2 shows a plot of the relative energetics and dissociation pathways for HOOOBr, HOOBrO, and their transition states. The reaction of the HO_2 and BrO radicals to produce the final products may proceed through the formation of either the HOOOBr or the HOOBrO intermediate. Our present calculations suggest that the most likely pathway is the formation of HOOBrO as an intermediate, which eventually dissociates into HOBr and O_2, since this process requires a very low energy barrier (2.8 kcal mol^{-1}). This is consistent with the earlier experimental observations[7,10] of HOBr being the predominant product of the BrO + HO_2 reaction pathway and the pressure-dependence studies which suggest a stable $HBrO_3$ complex. If the HOOOBr intermediate is formed, it will, most likely, dissociate into HBr and O_3, but the energy barrier involved in this process is much higher (23.8 kcal mol^{-1}) than the barrier for the HOOBrO → HOBr + O_2 dissociation process. It would be very unlikely for HOOOBr to dissociate into HOBr and O_2, since the energy barrier for the formation of HOBr + O_2 from the dissociation of HOOOBr is even higher (26.4 kcal mol^{-1}).

IV. Conclusion

The equilibrium structures, vibrational and electronic spectra, and relative energetics of the stable $HBrO_3$ isomers (HOOOBr and HOOBrO) and the HOOOBr → HOBr + O_2, HOOOBr → HBr + O_3, and HOOBrO → HOBr + O_2 transition states have been investigated with the QCISD *ab initio* electronic-structure method. The HOOBrO (or HOOOBr) intermediate species can be formed during the reaction of HO_2 radicals with BrO. The final products of the HO_2 + BrO reaction, HOBr and O_2, are very likely to result from the dissociation of the HOOBrO intermediate, which is the most energetically favored pathway.

References and Notes

(1) Anderson, J. G.; Toohey, D. W.; Brune, W. H. *Science* **1991**, *251*, 39.

(2) Salawitch, R. J.; McElroy, M. B.; Yatteau, J. H.; Wofsy, S. C.; Schoeberl, M. R.; Lait, L. R.; Newman, P. A.; Chan, K. R.; Loewenstein, M.; Podolske, J. R.; Strahan, S. E.; Proffitt, M. H. *Geophys. Res. Lett.* **1990**, *17*, 561.

(3) Yung, Y. L.; Pinto, J. P.; Watson, R. T.; Sander, S. P. *J. Atmos. Sci.* **1980**, *37*, 339.

(4) WMO. "Scientific Assessment of Ozone Depletion"; National Aeronautics and Space Administration, 1994.

(5) Cox, R. A.; Sheppard, D. W. *J. Chem. Soc., Faraday Trans. 2* **1982**, *78*, 1383.

(6) Baulch, D. L.; Cox, R. A.; Hampton, Jr., R. F.; Kerr, J. A.; Troe, J.; Watson, R. T. *J. Phys. Chem. Ref. Data* **1980**, *9*, 295.

(7) Poulet, G.; Pirre, M.; Maguin, F.; Ramaroson, R.; Le Bras, G. *Geophys. Res. Lett.* **1992**, *19*, 2305.

(8) Hayman, G. D.; Danis, F.; Thomas, D. H.; Peeters, J. Air Pollution Report No. 45, Commission of the European Communities, Brussels, 1993.

(9) Bridier, I.; Veyret, B.; Lesclaux, R. *Chem. Phys. Lett.* **1993**, *201*, 563.

(10) Larichev, M.; Maguin, F.; Le Bras, G.; Poulet, G. *J. Phys. Chem.* **1995**, *99*, 15911.

(11) Elrod, M. J.; Meads, R. F.; Lipson, J. B.; Seeley, J. V.; Molina, M. J. *J. Phys. Chem.* **1996**, *100*, 5808.

(12) Cronkhite, J. M.; Stickel, R. E.; Nicovich, J. M.; Wine, P. H. *J. Phys. Chem. A* **1998**, *102*, 6651.

(13) Mellouki, A.; Talukdar, R. K.; Howard, C. J. *J. Geophys. Res.* **1994**, *99*, 22949.

(14) Garcia, R. R.; Solomon, S. *J. Geophys. Res.* **1994**, *99*, 12937.

(15) Li, Z.; Friedl, R. R.; Sander, S. P. *J. Chem. Soc., Faraday Trans.* **1997**, *93*, 2683.

(16) Guha S.; Francisco, J. S. *J. Phys. Chem. A* **1998**, *102*, 2072.

(17) Frisch, M. J.; Trucks, G. W.; Schlegel, H. B.; Gill, P. M. W.; Johnson, B. G.; Robb, M. A.; Cheeseman, J. R.; Keith, T.; Petersson, G. A.; Montgomery, J. A.; Raghavachari, K.; Al-Laham, M. A.; Zakrzewski, V.; Ortiz, J. V.; Foresman, J. B.; Cioslowski, J.; Stefanov, B. B.; Nanayakkara, A.; Challacombe, M.; Peng, C. Y.; Ayala, P. Y.; Chen, W.; Wong, M. W.; Andres, J. L.; Replogle, E. S.; Gomperts, R.; Martin, R. L.; Fox, D. J.; Binkley, J. S.; Defrees, D. J.; Baker, J.; Stewart, J. P.; Head-Gordon, M.; Gonzales, C.; Pople, J. A. *GAUSSIAN 94*, Revision D.2; Gaussian, Inc.: Pittsburgh, PA, 1995.

(18) Pople, J. A.; Head-Gordon, M.; Raghavachari, K. *J. Chem. Phys.* **1987**, *87*, 5968.

(19) Krishnan, R.; Binkley, J. S.; Seeger, R.; Pople, J. A. *J. Chem. Phys.* **1980**, *72*, 650.

(20) Guha, S.; Francisco, J. S. *J. Phys. Chem. A* **1997**, *101*, 5347.

(21) Francisco, J. S.; Sander, S. P. *J. Phys. Chem.* **1996**, *100*, 573.